Chemical Physics Letters 582 (2013) 21–23

Contents lists available at ScienceDirect

Chemical Physics Letters

journal homepage: www.elsevier.com/locate/cplett

Photoelectron spectroscopic study of the ethyl cyanoacrylate anion

Xinxing Zhang, Xin Tang, Kit Bowen *

Department of Chemistry, Johns Hopkins University, 3400 N. Charles Street, Baltimore, MD 21218, USA

ARTICLE INFO

Article history:
Received 5 June 2013
In final form 17 July 2013
Available online 24 July 2013

ABSTRACT

Anion photoelectron spectroscopy and density functional theory have been utilized to study the parent, ethyl cyanoacrylate molecular anion, ECA^-. The measured electron affinity (0.9 ± 0.2 eV), vertical detachment energy (1.3 ± 0.1 eV), and anion-to-triplet neutral, photodetachment transition energies (4.0 ± 0.1 eV and 4.5 ± 0.1 eV) all compare well with their calculated values. The relatively high electron affinity of the ECA monomer is responsible for the fact that its "anionic" polymerization mechanism proceeds even with weak nucleophiles, such as water.

1. Introduction

Ethyl cyanoacrylate (ECA) polymerizes rapidly in the presence of atmospheric moisture [1,2]. ECA is the principal component of the commercial glues, Super-Glue and Krazy-Glue. Since ECA polymerizes so readily, there are relatively few studies of its monomer, although both Raman and infrared spectroscopic studies [3–5] as well as adhesive layer electron tunneling studies have been reported [6].

ECA polymerizes through a classic "anionic" polymerization mechanism, in which a nucleophile attacks its β-unsaturated carbon and forms a carbanion (see Figure 1). The resulting carbanion then attacks another monomer and propagates the polymerization reaction [7]. Compared to other monomers, such as butadiene and styrene, which also polymerize via an anionic mechanism, ECA exhibits a much higher rate of polymerization [8]. This is due to ECA having both –CN and –COO– electron-withdrawing groups bonded to its α-C; they stabilize the resulting carbanion [8]. As a result, even weak nucleophilic initiators, such as water, are able to induce rapid polymerization in ECA [8].

The polymerization of ECA described above is consistent with a density functional theory (DFT) study by Teng et al. [9]. These authors proposed a correlation between the adiabatic electron affinity (EA) value of a given monomer and the rapidity of its anionic polymerization. They found that monomers with EA values less than about 0.2 eV undergo anionic polymerization only with strong nucleophilic initiators, whereas monomers with EA values over 0.6 eV polymerize even with very mild nucleophiles. Their calculations predicted the EA value of ECA to be 1.0 eV, which is substantially higher than that of most other common monomers [9]. Their work underscored the importance of monomer electron affinities in anionic polymerization.

In the present letter, we measured the anion photoelectron spectrum of the ECA parent anion, ECA^-, and performed DFT calculations on both ECA and its anion. Our calculations provided the EA value of ECA, the vertical detachment energy (VDE) of ECA^-, and the photodetachment transitions energies to two triplet, excited states of neutral ECA. These computational results were used to assign the photoelectron spectrum.

2. Experimental and computational methods

Anion photoelectron spectroscopy is conducted by crossing a mass-selected beam of negative ions with a fixed-frequency photon beam and energy-analyzing the resultant photodetached electrons. It is governed by the energy-conserving relationship, $h\nu = EBE + EKE$, where $h\nu$ is the photon energy, EBE is the electron binding (transition) energy, and EKE is the electron kinetic energy. Our anion photoelectron spectrometer, which has been described previously, [10] consists of a laser vaporization anion source, a linear time-of-flight mass analyzer/selector, a pulsed Nd:YAG photodetachment laser (0.4–0.5 mJ per pulse into ~1 mm^2), and a magnetic bottle electron energy analyzer. Photoelectron spectra were calibrated against the well-known photoelectron spectrum of Cu^- [11]. Parent anions of ethyl cyanoacrylate, ECA^-, were generated in a modified, laser vaporization source. Several drops of ECA were coated onto a copper disk, and then polymerized to form a solid layer. The coated disk was then ablated by a pulsed Nd:YAG laser beam operating at a wavelength of 532 nm. The resulting plasma was cooled by supersonically expanding a plume of helium gas from a pulsed gas valve (backing pressure of ~100 psi) directly over the disk. Negatively charged anions were then extracted into the spectrometer prior to mass selection and photodetachment.

DFT calculations were conducted by applying Becke's three-parameter hybrid functional (B3LYP) [12–14] using the GAMESS software package [15,16] to determine the EA value of ECA, the VDE value of ECA^-, and the photodetachment transition energies

* Corresponding author. Fax: +1 410 516 8420.
E-mail address: kbowen@jhu.edu (K. Bowen).

0009-2614/$ - see front matter © 2013 Elsevier B.V. All rights reserved.
http://dx.doi.org/10.1016/j.cplett.2013.07.041

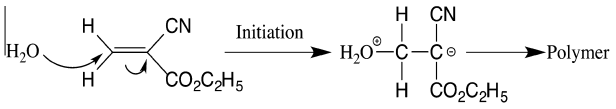

Figure 1. Classic "anionic" polymerization mechanism in which nucleophilic attack yields a carbanion, here drawn for the case of ECA.

of the excited states observed in the spectrum of ECA^-. The B3LYP method has been found to be satisfactory for predicting excess electron-binding energies for many molecular valence anions [17]. All geometries, including that of the anion and its corresponding neutral molecule, were fully optimized without any geometrical constraints while using the aug-cc-pVDZ basis set [18]. The electronic energies were improved by single-point calculations with a larger basis set, i.e., aug-cc-pVTZ, at optimized geometries [19]. The energies for the excited triplet and singlet states of the neutral molecule were calculated with time-dependent DFT methods, using the aug-cc-pVTZ basis set [20–22].

3. Results

Two photoelectron spectra of the ECA^- molecular anion are shown in Figure 2a and b, these having been recorded with 355 nm (3.49 eV) and 266 nm (4.66 eV) photons, respectively. Several bands are observed. Since the ECA^- anion is a doublet, photodetachment transitions can occur from it to both singlets and triplets of neutral ECA. The transition from the ECA^- doublet, ground state anion to the singlet, ground state of neutral ECA is denoted as the S_0 band in both Figure 2a and b, whereas transitions from the ECA^- anion to the first and second triplet, excited states of neutral ECA are denoted as T_1 andT_2 bands in Figure 2b.

The adiabatic electron affinity, EA, is the energy difference between the lowest energy, vibronic state of the anion and the lowest energy, vibronic state of its neutral counterpart. Assuming significant Franck–Condon overlap between $v = 0$ of the anion and $v' = 0$ of its corresponding neutral (the origin transition), the EA value will be contained within the transitions of the S_0 band. Furthermore, if no vibrational hot bands (photoelectrons from vibrationally excited anions) were to be present, then the EBE value of the intensity threshold would correspond to the EA value. However, depending on the anion and the source by which it was generated, it is not uncommon for some degree of vibrational hot band intensity to be present. Taking this possibility into account, we have determined the EA of ECA by extrapolating the low EBE side of the S_0 band to zero, with the corresponding EBE value there being taken as the EA. Thus, we have determined the EA of ECA to be 0.9 ± 0.2 eV. Our calculated value of EA is 0.88 eV, in excellent agreement with our experimentally-determined value and in good accord with the previously calculated value of 1.0 eV [9].

The EBE value at the intensity maximum of the S_0 band is the vertical detachment energy, VDE, i.e., the transition energy at which the Franck Condon overlap between the wave functions of the anion and its neutral counterpart is maximal. We have determined the VDE value for ECA^- to be 1.3 ± 0.1 eV. Our calculated value of VDE is 1.29 eV, in excellent agreement with our experimentally-determined value.

We also carried out a Franck–Condon analysis of the S_0 band using PESCAL2010 software [23]. Figure 3 compares the fit that we obtained with the S_0 band profile seen in Figure 2a. Agreement between their overall shapes is very good and no significant vibrational hot bands are in evidence. The spacings between peaks (~0.27 eV) in the calculated band profile is predominately due to the C–N stretch. While there is only faint evidence of these peaks in the actual spectrum; they can be located by vertical dotted lines connecting them in Figure 3.

Figure 2b exhibits two or more features beyond the S_0 band. These were assigned with the aid of our computations. We calculated photodetachment transition energies from the ECA^- anion to two triplet and one singlet, excited states of neutral ECA. Since the calculated transition energy from the ground state of the ECA^- anion to the first excited triplet state of the neutral molecule (T_1) is 3.99 eV, we assign the spectral feature at EBE = 4.0 eV to that transition. Likewise, since the calculated transition energy from the ground state of the ECA^- anion to the second excited triplet state of the neutral molecule (T_2) is 4.73 eV, we assign the spectral features at EBE ~4.5 eV to that transition. Compared to the T_1 peak, the T_2 feature is much stronger; it is also composed of two vibrationally-resolved peaks, which are separated by ~0.17 eV. We assign this vibration to the in-plane deformation of the $=CH_2$ group (~1380 cm^{-1}) [3,6]. Our calculations also predicted a transition at EBE = 5.02 eV to occur from the ECA^- anion to the first ex-

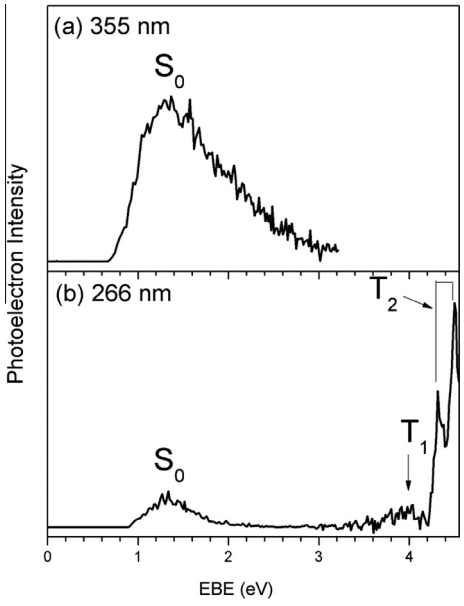

Figure 2. Anion photoelectron spectra of the ECA^- parent anion measured with both (a) 355 nm [3.49 eV] and (b) 266 nm [4.66 eV] photons.

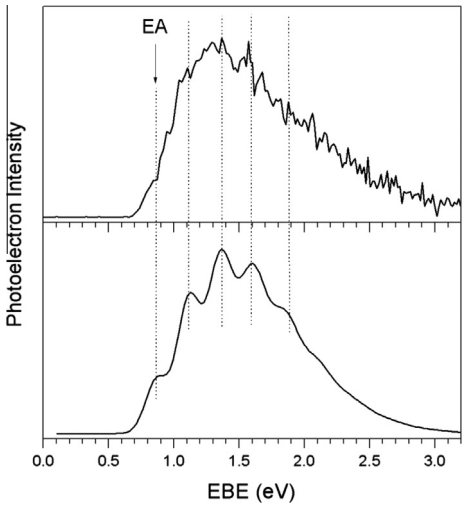

Figure 3. Comparison of measured (upper) and simulated (lower) S_0 band profiles of the ECA^- photoelectron spectrum.

Table 1
Measured and computed values of the electron affinity (EA) of ECA, the vertical detachment energy (VDE) of ECA$^-$, and in addition, the photodetachment transition energies from the ECA$^-$ anion to the T_1, T_2, and S_1 states of neutral ECA. All the numbers are in units of eV.

States		Expt.	Theo.
S_0	EA	0.9	0.88
	VDE	1.3	1.29
T_1		4.0	3.99
T_2		4.5	4.73
S_1		–	5.02

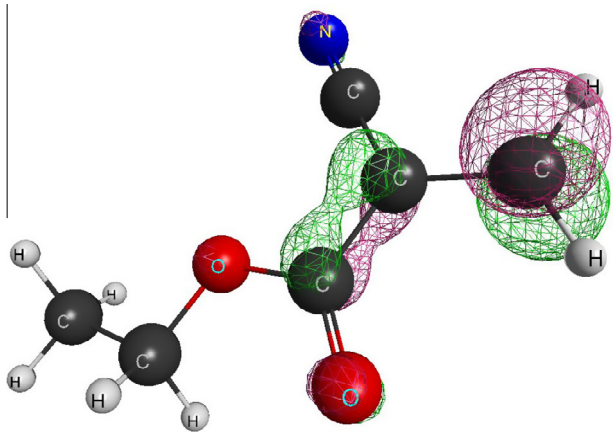

Figure 4. Depiction of the highest-filled molecular orbital of ECA$^-$ anion, showing that the excess electron is delocalized and occupies the π^* anti-bonding orbital.

cited singlet state (S_1) of neutral ECA. This transition, however, was not observed, since it would occur beyond the photon energy that we used to measure the ECA$^-$ photoelectron spectrum. Table 1 presents comparisons between the experimental and the calculated values measured and computed during this letter.

4. Discussion

The proposed correlation between the adiabatic electron affinity (EA) value of a given monomer and the ease of its anionic polymerization [9] deserves additional comment. Many monomers that polymerize via the anionic mechanism have negative EA values, and in those cases strong nucleophiles are required to initiate polymerization. Examples of monomers in this category are styrene, butadiene, and 1,3-cyclohexadiene. However, other monomers have relatively high EA values, due to their strong electron-withdrawing groups, and these polymerize even with weak nucleophiles. Examples of monomers in this category are nitroethylene (EA = 1.2 eV) [24,25] and ECA (EA = 0.9 eV). Higher EA values appear to enhance polymerization because of their ability to stabilize excess electrons.

As shown in Figure 1, in the traditional anionic polymerization mechanism, the β-carbon is no longer part of the π-conjugate system after initiation. In the case of the ECA$^-$ anion, however, our calculations show that the anion retains a planar CH_2=C(CN)COO– structure within a π-conjugate system, just as in the neutral molecule (see Figure 4). There, the excess electron is delocalized and occupies the π^* anti-bonding orbital. Thus, if one were to start with ECA$^-$ anions, rather than with neutral ECA molecules, the polymerization mechanism might well proceed differently.

There is some precedent for this. Electron beam irradiation is known to promote the curing of polymers. Using electron transmission and electron energy-loss techniques to study the anions of gas phase methyl–acrylate and methyl–methacrylate, Schafer et al. [26] proposed that their monomers can capture thermalized electrons during electron beam irradiation to give radical anions. These anions were then thought to obtain protons from ambient water molecules to form free radicals, inducing polymerization via a free radical mechanism. We extend this approach to ECA$^-$ anions. If enough of them could be created in the condensed phase, ECA's polymerization might also be enticed to follow an alternative, free radical mechanism (see Figure 5). In addition to electron beam irradiation of ECA films as a methodology for initiating a free radical mechanism, the introduction of alkali metal into batches of ECA might also have the same effect, since alkali metals are known to initiate polymerization in other systems by free radical mechanisms.

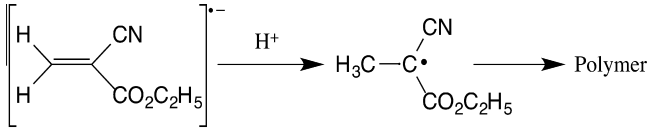

Figure 5. Free radical polymerization mechanism, here drawn for the case of the ECA$^-$ anion.

Acknowledgement

This material is based upon work supported by the National Science Foundation under Grant No. CHE-1111693 (KHB).

Appendix A. Supplementary data

Supplementary data associated with this article can be found, in the online version, at http://dx.doi.org/10.1016/j.cplett.2013.07.041.

References

[1] H.W. Coover, D.W. Dreifus, J.T. O'Connor, Handbook of Adhesives, Van Nostrand Reinhold, New York, 1990.
[2] G.H. Millett, Structural Adhesives: Chemistry and Technology, Plenum Press, New York, 1986.
[3] H.G.M. Edwards, J.S. Day, J. Raman Spectrosc. 35 (2004) 555.
[4] E. Urlaub, J. Popp, V.E. Roman, W. Kiefer, M. Lankers, G. Rössling, Chem. Phys. Lett. 298 (1998) 177.
[5] M. Asquier, P. Colomban, V. Milande, J. Raman Spectrosc. 40 (2009) 1641.
[6] S. Reynolds, D.P. Oxley, R.G. Pritch, Spectrochim. Acta 38A (1982) 103.
[7] D.C. Pepper, Macromol. Chem. Macromol. Symp. 60 (1992) 267.
[8] H. Hsieh, R. Quirk, Anionic Polymerization: Principles and Practical Applications, Marcel Dekker, Inc., New York, 1996.
[9] B. Teng, S. Jiang, J. Lu, Y. Lan, Y. Liu, S. Zheng, Acta Polym. Sin. 1 (2007) 1183.
[10] M. Gerhards, O.C. Thomas, J.M. Nilles, W.J. Zheng, K.H. Bowen, J. Chem. Phys. 116 (2002) 10247.
[11] J. Ho, K.M. Ervin, W.C. Lineberger, J. Chem. Phys. 93 (1990) 6987.
[12] A.D. Becke, Phys. Rev. A 38 (1988) 3098.
[13] A.D. Becke, J. Chem. Phys. 98 (1993) 5648.
[14] C. Lee, W. Yang, R.G. Parr, Phys. Rev. B 37 (1988) 785.
[15] M.W. Schmidt et al., J. Comput. Chem. 14 (1993) 1347.
[16] M.S. Gordon, M.W. Schmidt, in: C.E. Dykstra, G. Frenking, K.S. Kim, G.E. Scuseria (Eds.), Theory and Applications of Computational Chemistry: The First Forty Years, Elsevier, Amsterdam, 2005, p. 1167.
[17] J.C. Rienstra-Kiracofe, G.S. Tschumper, H.F. Schaefer, S. Nandi, G.B. Ellison, Chem. Rev. 102 (2002) 231.
[18] D.E. Woon, T.H. Dunning Jr., J. Chem. Phys. 90 (1989) 1007.
[19] D.E. Woon, T.H. Dunning Jr., J. Chem. Phys. 98 (1993) 1358.
[20] M.A.L. Marques, E.K.U. Gross, Annu. Rev. Phys. Chem. 55 (2004) 427.
[21] K. Burke, J. Werschnik, E.K.U. Gross, J. Chem. Phys. 123 (2005) 062206.
[22] M.E. Casida, M. Huix-Rotllant, Annu. Rev. Phys. Chem. 63 (2012) 287.
[23] K.M. Ervin, J. Ho, W.C. Lineberger, J. Phys. Chem. 92 (1988) 5405.
[24] H. Yamaoka, F. Williams, K. Hayashi, Trans. Faraday Soc. 63 (1967) 376.
[25] R. Vianello, N. Peran, Z.B. Maksić, Eur. J. Org. Chem. 2007 (2007) 526.
[26] Olivier Schafer, M. Allan, E. Haselbach, R.S. Davidson, Photochem. Photobiol. 50 (1989) 717.